JOURNAL OF GEOPHYSICAL RESEARCH, VOL. 103, NO. D15, PAGES 19,173–19,182, AUGUST 20, 1998

Stratosphere–troposphere exchange of ozone associated with the equatorial Kelvin wave as observed with ozonesondes and rawinsondes

Masatomo Fujiwara, Kazuyuki Kita, and Toshihiro Ogawa[1]

Department of Earth and Planetary Physics, Graduate School of Science, University of Tokyo, Tokyo

Abstract. An intensive observation with ozonesondes and rawinsondes was conducted in Indonesia in May and June 1995 to investigate a phenomenon of ozone enhancement in the tropical upper troposphere. We obtained the characteristics of an enhancement that continued for about 20 days, concurring with a zonal wind oscillation associated with the equatorial Kelvin wave around the tropopause and the Madden-Julian oscillation (MJO) in the troposphere. The isoline of ozone mixing ratio of 40 nmol/mol moved by 5.0 km downward from 17.8 km to 12.8 km, while the tropopause height was 16.2-17.8 km throughout the period. Moreover, the maximum ozone concentration of 300 nmol/mol at the tropopause was concurrent with the maximum eastward wind phase of the Kelvin wave. The detailed mechanism of the ozone transport is interpreted as follows: The downward motion associated with the Kelvin wave and the MJO transported the stratospheric ozone into the troposphere, and the air mixing due to the Kelvin wave breaking at the tropopause also caused stratosphere-troposphere exchange. The upper limit of the net amount of ozone transported from the stratosphere was estimated to be 9.9 Dobson units with the zonal and meridional extents of the ozone-increased region of more than 6.6×10^6 m and 1.8×10^6 m, respectively, to imply the potential to affect the photochemistry around the tropical tropopause.

1. Introduction

Recently, the significance of tropospheric ozone in the tropics has been recognized in terms of the oxidizing efficiency and greenhouse effect, and various efforts have been made to investigate its spatial distribution and temporal variation [*Kley et al.*, 1996; *Thompson et al.*, 1997; *Crutzen and Lawrence*, 1997]. However, especially in the upper troposphere, the ozone budget in the tropics has not been fully understood yet because of the sparsity of the ground-based and long-term observations.

We have been conducting a regular ozonesonde sounding at Watukosek (7.5°S, 112.6°E), Indonesia (Figure 1), since 1993 in collaboration with the Indonesian National Institute of Aeronautics and Space (LAPAN) and the National Space Development Agency of Japan (NASDA). The previous data analysis revealed that a phenomenon of large ozone enhancement in the upper troposphere, altitudes of 12-16 km, sometimes occurred in April, May, and June during the transition period from the local wet season to the dry one [*Komala et al.*, 1996]. Two possible explanations for this phenomenon were mentioned: (1) the long-range transport of ozone and ozone precursor gases originating from biomass burning in the Asian continent where it is at the end of the local dry season and (2) the downward transport from the stratosphere by a certain mechanism of the stratosphere-troposphere exchange (STE) such as the deformation of the tropopause by the equatorial Kelvin wave activity, as suggested by *Tsuda et al.* [1994a]. It should be noted that the phenomenon tends to be observed when both biomass burning and convection, the latter of which may also increase ozone through lightning or transport of ozone-rich air from the surface, are not so active in Indonesia.

Other previous reports related to the ozone enhancement in the tropical upper troposphere are available as follows: *Pickering et al.* [1993] discussed the role of lightning-produced NO_x in the active convective system as a source of the upper tropospheric ozone. *Diab et al.* [1996] presented time-height cross sections of tropospheric ozone at four ozonesonde stations located in southern Africa and the tropical Atlantic Ocean during the Southern African Fire-Atmosphere Research Initiative (SAFARI-92) period. They interpreted the upper tropospheric ozone enhancements observed at Brazzaville, Congo, and Ascension Island as a result of stratosphere-troposphere exchange with analyses of vertical wind and potential vorticity. *Kley et al.* [1996] showed the results from several ozonesonde observations over the tropical Pacific in March 1993, mentioning that the elevated ozone concentrations in the upper troposphere observed over Christmas Island were due to the stratospheric

[1]Now at Earth Observation Research Center, National Space Development Agency of Japan, Tokyo

Paper number 98JD01419.
0148-0227/98/98JD-01419$09.00

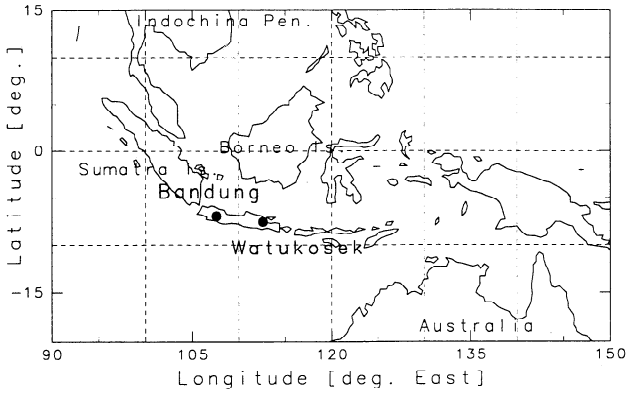

Figure 1. The locations of the observational sites, Watukosek (7.5°S, 112.6°E) and Bandung (6.9°S, 107.6°E).

influx. *Weller et al.* [1996] constructed meridional cross sections of tropospheric ozone over the Atlantic with the ozonesonde observation aboard a research vessel, showing a large ozone enhancement in the tropical upper troposphere in May and June 1994. *Folkins et al.* [1997] analyzed the enhancement of upper tropospheric NO, NO_y, CO, and ozone observed during an aircraft campaign over Fiji in the central tropical Pacific in October 1994. Since the enhanced air mass originated as outflow from a convective disturbance near New Guinea, they ascribed it to the extensive biomass burning that occurred in October 1994 in Indonesia. *Suhre et al.* [1997] reported several episodes of very high concentration of ozone over the Atlantic as observed by a specially equipped commercial aircraft. However, the observations of the ozone enhancement in the tropical upper troposphere are still too limited to understand the photochemical and dynamical characteristics of the phenomenon comprehensively.

An intensive observation was conducted in May and June 1995 with 11 ozonesonde soundings at Watukosek and more than one rawinsonde sounding per day at Bandung (6.9°S, 107.6°E; 600 km west of Watukosek), Indonesia. In this paper, we present the results of the observation that revealed several characteristics of the ozone enhancement concurring with the equatorial Kelvin wave activity around the tropopause and the Madden-Julian oscillation in the troposphere (sections 2 and 3) and interpret the transport mechanism. Detailed processes of the ozone transport are discussed in section 4. Net amount of ozone transported from the stratosphere is estimated in section 5. Discussion and conclusions are in sections 6 and 7.

2. Observation

The vertical distributions of atmospheric ozone concentration and temperature were measured by Meisei RSII-KC79D electrochemical carbon-iodine ozonesondes with TX3000-type TOTEX balloons and a tracking system at Watukosek. The observations were successfully conducted on May 3, 9, 17, 22, 26, 29, and 30 and June 1, 3, 5, and 14. Though five other soundings were also conducted during the period, we did not use them in the analysis because the data were not of good quality due to malfunction of the ozonesonde or the receiver or abrupt power failure of the station. The data sampling times are 4 seconds for ozone and 16 seconds for the other parameters with an ascending speed of ~5 m s^{-1}. In this paper, the vertical resolution is set to 200 m. The vertical distributions of horizontal wind and atmospheric temperature were measured with Vaisala RS-80 rawinsondes at Bandung [cf. *Shimizu and Tsuda,* 1997]. We use the profiles obtained at 0700 LST during the period between May 1 and June 15 with a vertical resolution of 150 m.

Six successive vertical distributions of ozone mixing ratio and temperature obtained at Watukosek illustrate that the tropopause defined by the minimum temperature was located around 16-18 km, whereas the ozone profile changed drastically near the tropopause (Figure 2). While the ozone

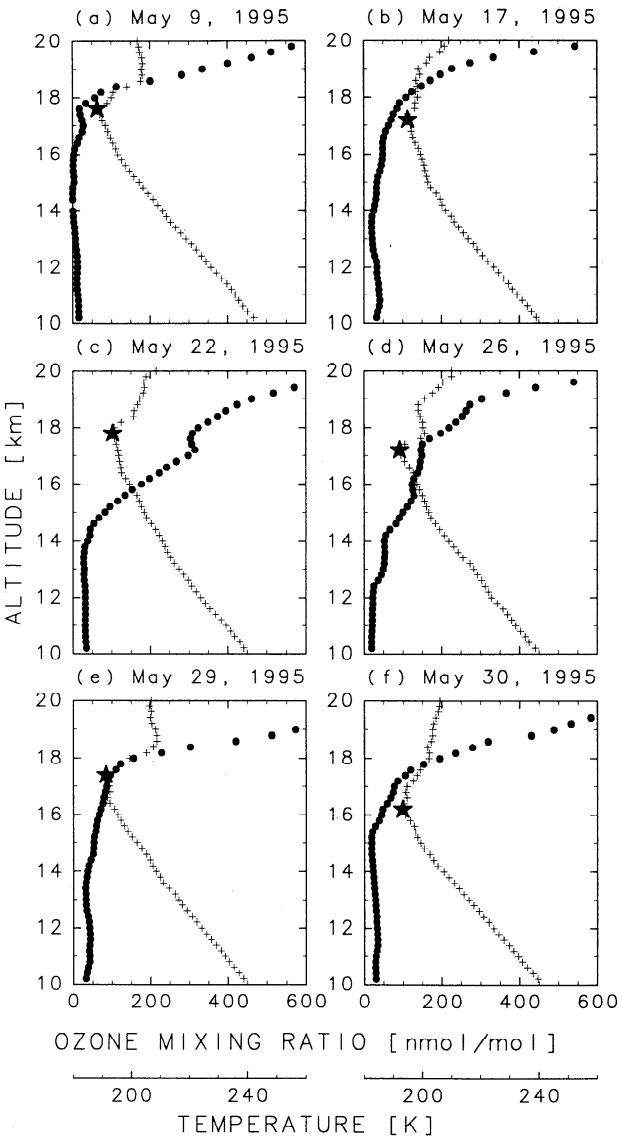

Figure 2. Vertical distributions of atmospheric ozone mixing ratio (solid circles) and temperature (crosses) in 10-20 km observed with ozonesondes at Watukosek on (a) May 9, (b) May 17, (c) May 22, (d) May 26, (e) May 29, and (f) May 30. The tropopause height defined by the minimum temperature is also indicated by a star in each panel.

mixing ratio increased rapidly with altitude just above the tropopause on May 9, the increase started at lower altitudes on May 17, 22, and 26. Between 17 and 18 km on May 22, a constant mixing ratio of ~300 nmol/mol (1 nmol/mol ≡ 1 ppbv) was observed, which was the maximum concentration at the tropopause during the observation period. Figure 3 shows the variation of vertical distribution of ozone mixing ratio at Watukosek. The isoline of 40 nmol/mol moved by 5.0 km downward from 17.8 km on May 9 to 12.8 km on May 26, while the tropopause was located around 16.2-17.8 km throughout the period. The 120 nmol/mol isoline also moved by 3.0 km downward from 18.4 km on May 9 to 15.4 km on May 26. On the other hand, while the 160-320 nmol/mol isolines moved downward from May 17 to May 22, they had recovered on May 26. After May 26, the 40-120 nmol/mol isolines in the upper troposphere had also recovered by June 1.

Figure 4 compares the variation of temperature profile at Watukosek with that at Bandung. The variations of the tropopause height at Watukosek and Bandung agree well if the difference of the time resolution is considered. Because the distance between the two sites is only 600 km with a small latitudinal difference, it can be assumed that the rawinsonde data at Bandung represent the meteorological situation at Watukosek in the case of large-scale phenomena.

Figure 5 shows the variation of potential temperature calculated from the rawinsonde data at Bandung. From May 11 to May 22, the isolines between 355 and 375 K moved downward. To investigate the vertical motion in detail, the variation of vertical distribution of potential temperature deviation from the time mean is plotted in Figure 6. The potential temperature deviation should be proportional to the downward displacement for adiabatic motions when the square of the Brünt-Väisälä frequency N (N^2) is constant. Large downward displacement at the tropopause, which had begun in the lower stratosphere, was seen on May 15 and 16 when the tropopause jumped. After that, between May 16 and May 29, a large region of downward displacement was seen in the upper troposphere, which nearly corresponded with the ozone-enhanced region in Figure 3. These results support the insight that the enhanced ozone in the upper troposphere originated from the higher altitudes, i.e., the stratosphere. However, it should be noted that the maximum ozone concentration at the tropopause appeared not on May 17 but on May 22, though the largest downward displacement at the tropopause was seen on May 15 and 16. Note also the concurrence of large positive deviation and downward displacement of ozone isolines in the lower stratosphere between May 29 and June 3.

Plate 1 shows the variation of vertical distribution of zonal wind at Bandung. It revealed an oscillation around the tropopause, between 15 and 19 km, and in the troposphere below 15 km in May. At 17 km, its period was 23 days (between May 5 and May 28), and its amplitude was 8-12

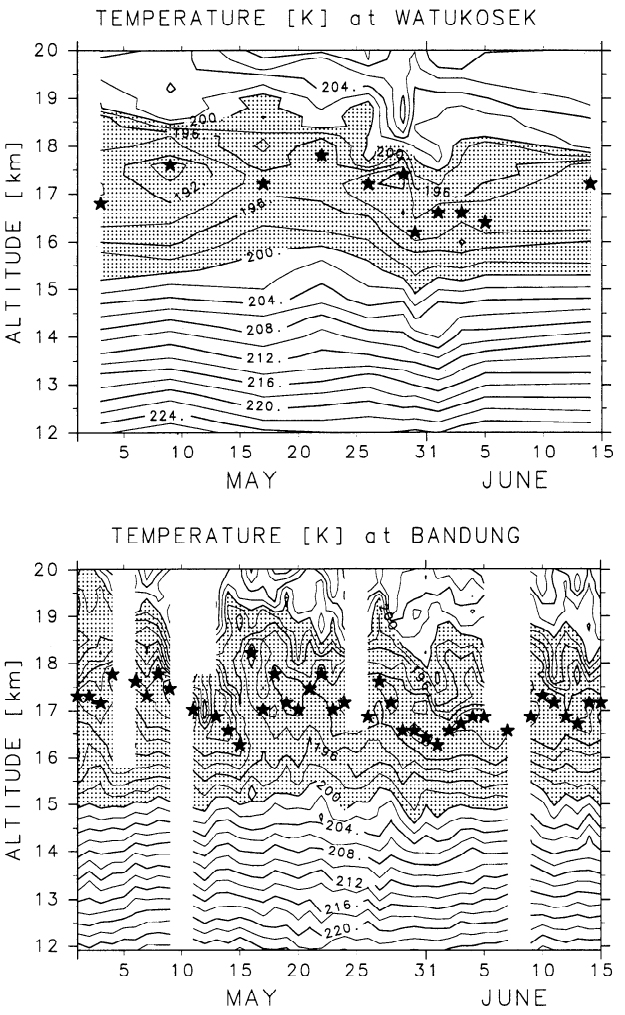

Figure 4. Variations of vertical distribution of atmospheric temperature at (top) Watukosek and (bottom) Bandung from May 1 to June 15. The contour interval is 2 K. The shaded regions correspond to those of less than 200 K. The tropopause height is also indicated at each station.

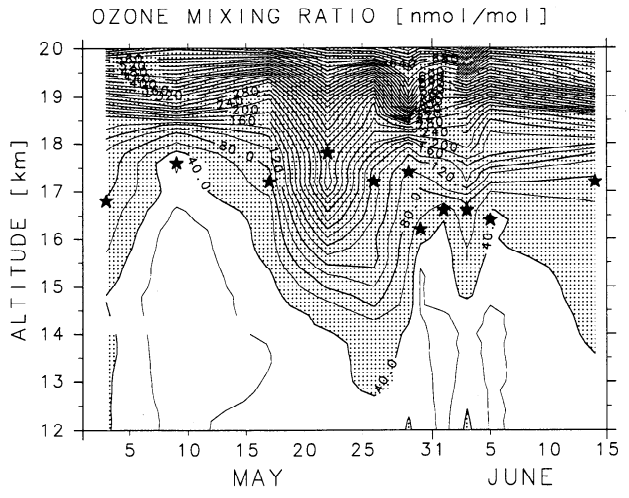

Figure 3. Variation of vertical distribution of ozone mixing ratio at Watukosek from May 3 to June 14 in 12-20 km. The contour interval is 20 nmol/mol. The shaded region corresponds to that of more than 40 nmol/mol. The tropopause height at Watukosek is also indicated.

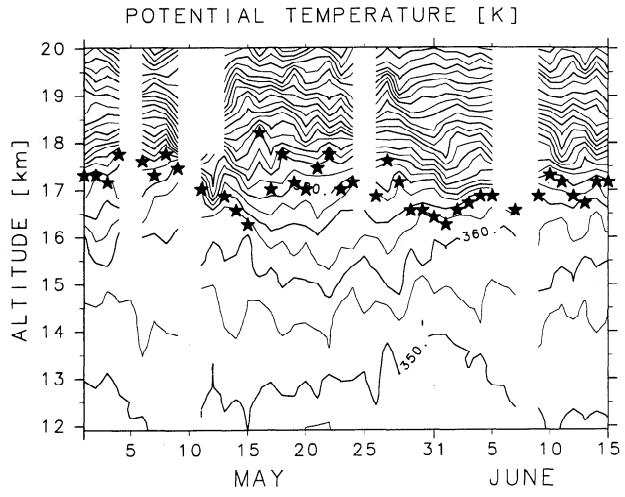

Figure 5. Variation of vertical distribution of potential temperature at Bandung. The contour interval is 5 K.

m s^{-1} on May 21 and 22. The isoline of 0 m s^{-1} moved downward from 18.5 km on May 9 to 14.8 km on May 22, with a corresponding vertical phase speed of -3.3×10^{-3} m s^{-1}. It should be noted that the maximum eastward wind phase at the tropopause appearing on May 21 and 22 was concurrent with the maximum ozone concentration at the tropopause observed on May 22. Below 14.8 km, the oscillation still existed till about 7 km (not shown), though the 0 m s^{-1} isoline was not tilting but rather vertical. The nature of the oscillation and its relation to the downward transport will be discussed in the following sections. The prevailing eastward wind above 19 km was associated with the eastward wind phase of the quasi-biennial oscillation (QBO). Figure 7 shows examples of vertical distributions of N^2 and atmospheric temperature at Bandung on May 15 and May 22. It can be seen that the representative values of N^2 in the lower stratosphere, at 15 km, and between 10 and 15 km are 5×10^{-4} s^{-2}, 1×10^{-4} s^{-2}, and 5×10^{-5} s^{-2}, respectively.

3. Analysis of the Observed Zonal Wind Oscillation

In this section, we investigate the nature of the zonal wind oscillation observed with the rawinsondes at Bandung. To examine the nature of the oscillation in broader horizontal extent, we use the zonal wind data of the global meteorological analysis by Japan Meteorological Agency (GANAL), whose horizontal grid is $1.875° \times 1.875°$ and whose vertical levels are surface, 1000, 850, 700, 500, 400, 300, 250, 200, 150, 100, 70, 50, 30, 20, and 10 hPa with a time resolution of 12 hours. Plate 2 represents the variation of zonal wind of GANAL along the 7.5°S latitude line on the 100-hPa level (~16 km altitude). The zonal wind oscillation with a period of about a month is seen in the eastern hemisphere, between 0° and 180° longitudes till the beginning of June. The region of the maximum eastward wind moves eastward with a speed of 8.9 m s^{-1} from 0° longitude on May 15 to 180° longitude on June 10. This eastward motion appears at altitudes from 300 hPa (~8.5 km) to 100 hPa. If the oscillation is interpreted as an eastward moving planetary-scale wave, the zonal phase speed relative to the ground $c^{(x)}$ is 8.9 m s^{-1}, and the spherical integer zonal wave number $s = ka \cos \phi$ is ~2, where k, a, and ϕ are zonal wave number, the radius of the Earth, and latitude, respectively. The background zonal wind on 100 hPa $\bar{u}$ is ~0 m s^{-1} in the eastern hemisphere. It should be noted that the phase, amplitude, vertical structure, and period of 26 days calculated from $2\pi/kc^{(x)}$ agree quite well with those observed with the rawinsondes at Bandung despite that the Bandung data were not used in GANAL. The characteristics of the zonal wind oscillation seen in both Plates 1 and 2 are summarized in Table 1.

The zonal wind oscillation above 14.8 km can be interpreted as the equatorial Kelvin wave, because its period is ~25 days; its vertical structure shows downward phase propagation; its horizontal structure is of planetary scale; and the system moves eastward. To confirm this interpretation, we calculate the vertical phase speed of the wave according to the linear theory of the equatorial Kelvin wave [*Andrews et al.*, 1987]. The dispersion relation of the Kelvin wave in the case of $\bar{u} = 0$ is written as

$$\omega = -Nk/m, \tag{1}$$

where ω is the frequency and m is the vertical wave number. Using $\omega \equiv kc^{(x)}$, the vertical wavelength λ_z and vertical phase speed $c^{(z)}$ are written as follows:

$$\lambda_z \equiv 2\pi/|m| = 2\pi|c^{(x)}|/N, \tag{2}$$

$$c^{(z)} \equiv \omega/m = -kc^{(x)2}/N. \tag{3}$$

Using the values of $c^{(x)}$ and k obtained from the GANAL analysis, λ_z and $c^{(z)}$ are estimated as shown in Table 2. Estimates of $c^{(z)}$ for the two altitude regions (~15 km and the lower stratosphere) have the same order of magnitude as

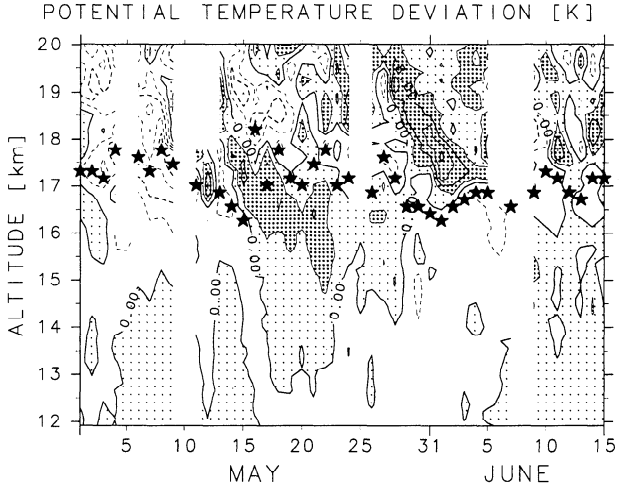

Figure 6. Variation of vertical distribution of potential temperature deviation at Bandung. The mean distribution is calculated from all the data in the observation period. The contour interval is 4 K. The lighter shaded regions correspond to those with positive values. The regions of more than +4 K are darker shaded.

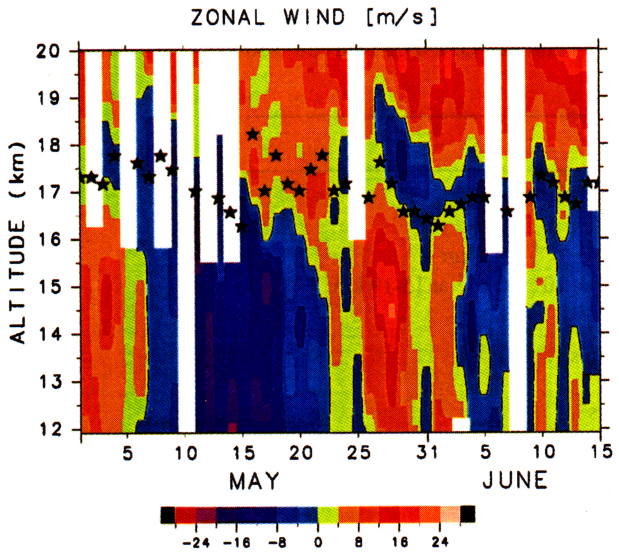

Plate 1. Variation of vertical distribution of zonal wind at Bandung.

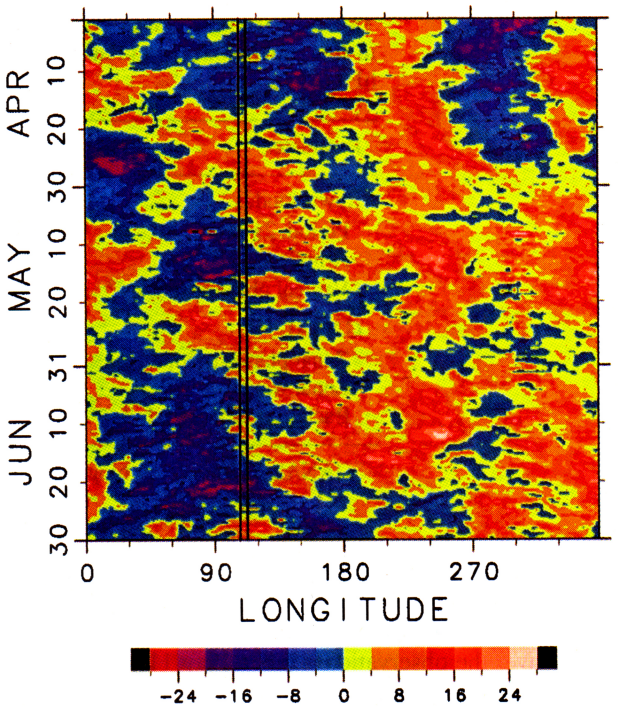

Plate 2. Variation of zonal wind along the 7.5°S latitude line on the 100-hPa level (~16 km altitude) from the GANAL data. The observational sites are indicated by lines.

that derived from the Bandung data (see Table 1), supporting the interpretation that the zonal wind oscillation seen in both Plates 1 and 2 is the equatorial Kelvin wave. Note that the observed $c^{(x)}$ (8.9 m s^{-1}) is much smaller than 25 m s^{-1} for the Kelvin waves frequently observed in the lower stratosphere [*Andrews et al.*, 1987].

On the other hand, the zonal wind oscillation still existed below 14.8 km, where the 0 m s^{-1} isolines are rather vertical (Plate 1). This is probably associated with the so-called Madden-Julian oscillation (MJO) [*Madden and Julian*, 1972], which is caused by the tropical hierarchical convective systems [*Nakazawa*, 1988]. To examine the convective activity during the observation period, we analyze the infrared equivalent blackbody temperature data by Japanese Geostationary Meteorological Satellite (GMS), whose horizontal grid is 1° × 1° with a time resolution of 3 hours. The temperature value represents the cloud top height, i.e., lower values correspond to taller clouds and vice versa. Plate 3

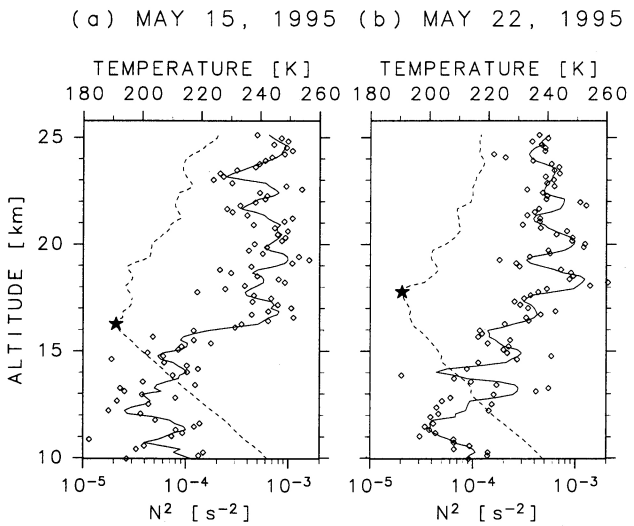

Figure 7. Vertical distributions of the square of the Brünt-Väisälä frequency N (diamonds and solid lines) and atmospheric temperature (dotted lines) with the tropopause (stars) in 10-26 km at Bandung on (a) May 15 and (b) May 22. The solid lines indicate the running averages of five data points.

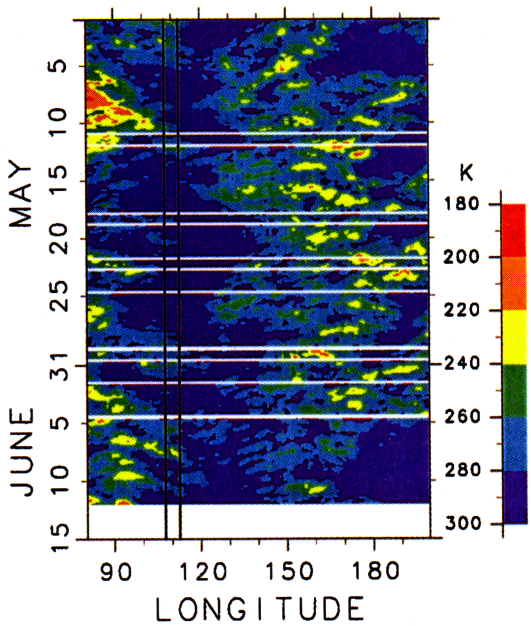

Plate 3. Variation of the infrared equivalent blackbody temperature, which represents the convective activity, along the latitudinal band between 5.5°S and 9.5°S from the Geostationary Meteorological Satellite data. The observational sites are indicated by lines.

Table 1. Summary of the Characteristics of the Zonal Wind Oscillation Seen in the Rawinsonde Data at Bandung (Plate 1) and the GANAL Data on 100 hPa (Plate 2)

Parameter	Value
Rawinsondes	
Period, $2\pi/kc^{(x)}$	23 days
Amplitude, U	8-12 m s^{-1} at 17 km
Vertical phase speed, $c^{(z)}$	-3.3×10^{-3} m s^{-1} at 15-19 km
GANAL	
Zonal phase speed, $c^{(x)}$	8.9 m s^{-1}
Zonal wave number, s	2
Background zonal wind, $\bar{u}$	0 m s^{-1}

GANAL, Japan Meteorological Agency.

shows the variation of the GMS data along the latitudinal band between 5.5°S and 9.5°S. It is revealed that an active large-scale convective system coming from the Indian Ocean passed over the observation sites on May 11, and after that, no remarkable system was observed till the beginning of June, which is consistent with the fact that the zonal wind direction changed from eastward to westward around May 8 (see Figures 16g and 16h of *Madden and Julian* [1972]).

4. Downward Transport of Ozone Associated With the Equatorial Kelvin Wave and MJO

In this section, we try to interpret the ozone variation in Figure 3 along with the concurrent prevailing meteorological feature around the tropopause, i.e., the equatorial Kelvin wave and the MJO in the troposphere. Three features in Figure 3 are focused on: the downward motion of the isolines of 40-120 nmol/mol from May 9 to May 26 (section 4.1); the occurrence of the maximum ozone concentration at the tropopause on May 22 (section 4.2); and the recovery of the isolines around the tropopause from May 22 to June 1 (section 4.3).

4.1. Downward Motion of Ozone Isolines From May 9 to May 26

Figure 8 is a schematic illustration of the wind perturbation (u', w') of the Kelvin wave, where u' and w' are the zonal and vertical wind components, respectively, and the isotherm, hence the material surface, deformed by the wave. According to this figure, the maximum downward displacement should occur during the transition period from the westward wind to the eastward one if one notes that this wave pattern moves eastward (During this period, the maximum of the Kelvin wave temperature component propagates downward through the average tropopause level. Thus the tropopause may jump if the wave amplitude is sufficiently large, as in the case of May 15-16, 1995 (Figure 5).). In fact, the deviation plot of potential temperature indicates this downward displacement as the regions of more than +4 K (Figure 6) corresponding to the downward motion of the 0 m s^{-1} isoline from May 9 to May 22 in Plate 1. According to Figure 5, +4 K change of potential temperature in the upper troposphere corresponds to 0.5-1.5 km downward displacement. To investigate whether the vertical extent is explained by adiabatic motions, we estimate the maximum vertical displacement $2\zeta_0$ associated with the Kelvin wave using the linear wave theory. The vertical wind component $w' = e^{z/2H} W \exp[i(kx + mz - \omega t)]$, where H (~7 km) is the scale height and W is the amplitude, can be expressed with the vertical displacement ζ' as $w' = \partial\zeta'/\partial t$ in the case of $\bar{u} = 0$. Substituting $\zeta' = e^{z/2H}\,\zeta_0 \exp[i(kx+mz-\omega t)+i\pi/2]$, where $\exp(i\pi/2)$ is the phase delay relative to w', and using the relation of the Kelvin wave's amplitudes, $W/U = -k/m$ (Figure 8) and equation (1), we obtain

$$\zeta_0 = U/N. \tag{4}$$

With $U = 10$ m s^{-1}, we calculate $2\zeta_0 = 2.0$ km at $N^2 = 1.0 \times 10^{-4}$ s^{-2} and $2\zeta_0 = 2.8$ km at $N^2 = 5.0 \times 10^{-5}$ s^{-2}. These results are consistent with those inferred from potential temperature deviation if one considers the maximum deviation of +8 K.

On the other hand, from May 9 to May 26, the ozone isoline of 40 nmol/mol moved by 5.0 km downward from the tropopause, and those of up to 120 nmol/mol also showed downward motions (Figure 3). Comparing the locations of these isolines in Figure 3 with the region of more than +4 K in the upper troposphere in Figure 6, most of their downward motion between May 9 and May 22 can be interpreted to have been due to the Kelvin wave. As for the further downward motion of the 40-120 nmol/mol isolines till May 26, the downward motion associated with the MJO may play a role.

Table 2. Estimated Values of λ_z and $c^{(z)}$ of the Equatorial Kelvin Wave at Given Values of N^2 and $c^{(x)} = 8.9$ m s^{-1}

	N^2, s^{-2}	
	1.0×10^{-4}	5.0×10^{-4}
λ_z, m	5.6×10^3	2.5×10^3
$c^{(z)}$, m s^{-1}	-2.5×10^{-3}	-1.1×10^{-3}

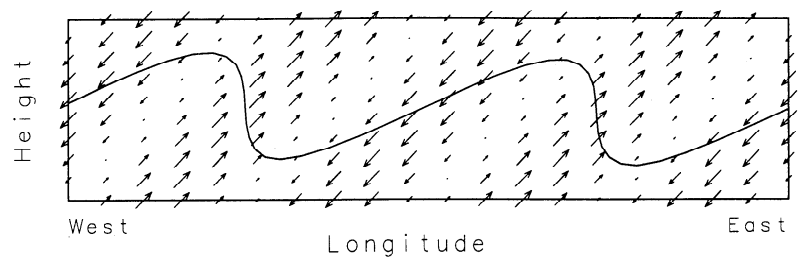

Figure 8. Schematic illustration of the wind perturbation (u', w') indicated by arrows associated with the equatorial Kelvin wave. The observer is moving eastward with the wave at the speed of $c^{(x)}$ relative to the ground. A hypothetical air parcel moves at a velocity of $(-c^+ + u', w')$ in this coordinate system, where $c^+ \equiv c^{(x)} - \bar{u}$. Its trajectory can be interpreted as the isotherm, hence the material surface, deformed by the wave. See the text for further discussions.

Around May 22 when the zonal wind direction changed from westward to eastward without any remarkable convection over Indonesia, the average vertical wind direction should have been downward, which corresponds to Figures 16b and 16c of *Madden and Julian* [1972]. *Holton* [1992] roughly estimated the speed of the subsidence balanced with the radiative cooling of 1 K day^{-1}, which is the typical value for the tropical nonconvective troposphere, as 3×10^{-3} m s^{-1}, which means that it takes 4 days to move by 1 km downward. This vertical speed is consistent with the motion of the 40 nmol/mol isoline from May 22 to May 26 in Figure 3.

4.2. Maximum Ozone Concentration at the Tropopause on May 22

Figure 3 also indicates that the maximum ozone concentration at the tropopause occurred on May 22 when the maximum eastward wind phase of the wave was observed (Plate 1), while the linear wave theory predicts its occurrence around May 16 because it was the transition period from the westward wind to the eastward one at the tropopause so that the maximum downward displacement should occur (Figure 8). Therefore any nonlinear process such as breaking of the wave should be considered to explain all the results of the observations consistently.

According to Table 1, the amplitude of the zonal wind component was comparable to the intrinsic zonal phase speed of the wave, $c^+ \equiv c^{(x)} - \bar{u}$, at the tropopause (i.e., $U \approx c^{(x)}$ as $\bar{u} = 0$ m s^{-1} at the tropopause). In such a case, the isotherm becomes vertical at least in the narrow region of the maximum eastward wind phase, as also illustrated in Figure 8, to generate a mixing region, in other words, breaking of a part of the wave occurs. The fact that a nearly constant mixing ratio of ~300 nmol/mol was observed between 17 and 18 km on May 22 (Figure 2) when the maximum eastward wind phase appeared at the tropopause (Plate 1) strongly suggests that the air mixing due to the wave breaking occurred around these altitudes. It should be noted that the small jumps of the tropopause at Bandung on May 21 and 22 may indicate the instability which had caused the air mixing around 17 km, as well as the existence of shorter-period waves [*Tsuda et al.*, 1994b; *Sato and Dunkerton*, 1997]. The enhanced ozone of more than 160 nmol/mol in the uppermost troposphere (above 16 km) on May 22 can be interpreted as the result of this mixing as well if one assumes that the breaking region had extended to these altitudes. As for the downward motion of the isolines more than 300 nmol/mol in the lowermost stratosphere between May 17 and May 22 (Figure 3), the downward phase propagation of the breaking region may play a role. The isolines more than 1280 nmol/mol (above 21.2 km) moved upward between May 17 and May 22 (not shown), which suggests that the enhanced ozone in the lowermost stratosphere had originated around 21.2 km.

Therefore the causes of the large ozone enhancement around the tropopause on May 22 can be summarized as follows: (1) The previous downward phase propagation of the air mixing region due to the wave breaking had increased the ozone concentration in the lowermost stratosphere; (2) on May 22, the breaking region had reached the tropopause and caused the ozone enhancement in the uppermost troposphere as well; and (3) the previous downward motion into the troposphere associated with the Kelvin wave and the MJO had increased the ozone concentration below 16 km, as discussed in the previous section.

4.3. Recovery of the Ozone Isolines From May 22 to June 1

After May 22, the ozone concentration in the uppermost troposphere had at least stopped increasing because the ozone transport from the stratosphere due to the Kelvin wave and its breaking had stopped as the maximum eastward wind phase had passed over Indonesia. For the recovery of the ozone isolines around the tropopause, we have two possibilities: One is the upward motion due to the Kelvin wave, and the other is the rapid horizontal mixing into the surrounding troposphere. The former is less plausible because Figure 6 shows only a small region of upward displacement across the tropopause during this period. It should be noted that the downward phase propagation of the Kelvin wave around the tropopause may result in less efficient upward transport than downward transport because it means that the downward transporting region moves downward into the less stable troposphere but the upward transporting region does not move upward. Thus most of the ozone molecules transported from the stratosphere had spread into the surrounding troposphere before they were transported back to the stratosphere.

5. Estimation of the Ozone Amount Transported Into the Troposphere

In this section, we roughly estimate the net amount of ozone transported from the stratosphere. According to the discussions in section 4, we can assume that the enhanced ozone on May 22 represented all the ozone molecules transported from the stratosphere between May 9 and June 1 and that most of them had remained in the troposphere. Ozone amounts between 12 km and the tropopause on May 9 and May 22 are 0.79 Dobson units (DU) (1 DU $\equiv 2.687\times10^{16}$ molecules of ozone cm^{-2}) and 10.64 DU, respectively, so that the increased ozone amount over Indonesia is estimated from the difference of the two as 9.9 DU. Note that this value is the upper limit. If one uses 7.56 DU for the same altitude region on May 26, one obtains a 6.8 DU increase. The meridional extent of the ozone-increased region, L_y, may be estimated from the approximate meridional scale of the equatorial waves as $L_y/2 \equiv (2N/\beta|m|)^{1/2}$, where $\beta \equiv 2\Omega a^{-1}$ cos ϕ and $\Omega \equiv 2\pi$(sidereal day)$^{-1}$ [*Andrews et al.*, 1987]. Putting appropriate values, we obtain $L_y = 1.8 \times 10^6$ m. On the other hand, the zonal extent, L_x, can be estimated from Plate 2 to be at least 6.6×10^6 m, corresponding to the region of large eastward wind between 60°E and 120°E around May 25. It should be noted that L_x will become larger if the nonbreaking regions, where ozone may be also transported into the troposphere irreversibly, are also included.

Total ozone in the tropics varies from 250 to 280 DU [*Fishman et al.*, 1990], and the ozone amount between 3 and 16 km at Watukosek varies from 10 to 25 DU [*Komala et al.*, 1996]. Thus the value of 9.9 (6.8) DU corresponds to 3.5-4.0% (2.4-2.7%) of total ozone and more than 40% (27%) of tropospheric ozone. Considering these facts and the horizontal extent of the ozone-increased region, the ozone transport associated with the Kelvin wave activity including wave breaking and the MJO has the potential to affect the photochemistry in the tropical troposphere. This phenomenon may be detectable with the satellite-borne total ozone mapping spectrometer (TOMS), though it might be difficult to exclude the perturbation component due to the Kelvin waves in the stratosphere [e.g. *Ziemke and Stanford*, 1994]. Unfortunately, the TOMS data are not available during our observation period.

6. Discussion

There are several possible origins for ozone enhancement in the tropical troposphere other than the stratosphere, such as biomass burning and lightning. Biomass burning is most prevalent at the end of the local dry season in September and October. Ozone is enhanced in the lower and middle troposphere due to the enhancement of ozone precursor gases, though no enhancement is seen in the upper troposphere at Watukosek even in these months between 1992 and 1995 [*Komala et al.*, 1996; *Fujiwara et al.*, 1996]. (However, large ozone enhancement throughout the troposphere was observed in September-December 1997, when the most active forest fire since the 1982-1983 period occurred in Indonesia.) On the other hand, lightning is most active in the local wet season between December and March, but the ozone concentration observed in Indonesia is the lowest (20-30 nmol/mol) throughout the troposphere in these months. There is also a possibility of the long-range transport of ozone or ozone precursor gases from distant biomass burning or lightning or from the stratosphere in midlatitudes. The former two may not enhance ozone in the upper troposphere over Indonesia except for the special cases such as the most active forest fire episode in 1997. The synoptic-scale wave activity in midlatitudes, which causes the ozone transport from the stratosphere, has no distinct seasonality in the southern hemisphere [*Trenberth*, 1991]. Therefore the phenomenon of the upper tropospheric ozone enhancement over Indonesia with a seasonality of April-June is mostly caused by the transport from the stratosphere associated with the equatorial wave activity.

The tropical stratosphere-troposphere exchange (STE) has been focused only on cumulonimbus penetration as a dehydration mechanism for the lowermost stratosphere, i.e., upward transport from the troposphere to the stratosphere since *Danielsen* [1982] proposed an intriguing hypothesis [*Russell et al.*, 1993; *Danielsen*, 1993; *Holton et al.*, 1995] (see also the special section on the NASA experiment on tropospheric-stratospheric water vapor transport in the Intertropical Convergence Zone (*Geophys. Res. Lett.*, *9*(6), 599-624, 1982)), though recently, some indirect cases in which the downward transport across the tropical tropopause may have had occurred were obtained [e.g., *Tsuda et al.*, 1994a; *Newell et al.*, 1996]. Our result suggests that the wave activity including wave breaking around the tropopause is a possible STE mechanism in the tropics. It should be noted that it would also affect the water vapor mixing ratio in the lowermost stratosphere in a different way from cumulonimbus penetration because the tropopause temperature fluctuation associated with wave disturbances is different from that with cumulonimbus penetration. Therefore the STE process associated with the equatorial waves must be studied comprehensively to estimate its influence on the photochemistry around the tropical tropopause.

For the above purpose, we need to know (1) the temporal and spatial variations of the wave activity including wave breaking around the tropical tropopause, (2) the relationship between the wave breaking at the tropopause and the background meteorological conditions in both the troposphere and the lowermost stratosphere, and (3) the amounts of constituents transported across the tropopause by waves including their breaking. As for case 1, some case studies [*Tsuda et al.*, 1994a, b; *Nishi and Sumi*, 1995; *Shimizu and Tsuda*, 1997] and statistical studies [*Maruyama*, 1991; *Sato et al.*, 1994; *Sato and Dunkerton*, 1997] have been made on the wave activity around the tropical tropopause. *Maruyama* [1991] showed that the Kelvin waves were most active in March on 70 hPa (~18.5 km altitude) over Singapore. Using the same data set with a shorter period, *Sato and Dunkerton* [1997] showed that the Kelvin waves with relatively small zonal phase speed reported by *Tsuda et al.* [1994a] were common around the tropopause, which was perhaps related to the long duration of eastward wind above the tropopause. It should be noted that all of them are based on the data set taken in the equatorial east Asia or the western Pacific. Further studies are crucially needed to investigate the global wave activity in terms of the cross-tropopause transport by analyzing the data from stations and global analyses. As

for cases 2 and 3, numerical experiments to characterize the transport should be made with regard to the wave parameters such as the zonal phase speed, amplitude of the zonal wind component, and zonal wave number along with the background meteorological conditions for zonal wind and temperature distributions. It should be noted that $\partial N^2/\partial z$ is very large in the uppermost troposphere so that the WKBJ approximation of the linear wave theory is no longer valid [cf. *Andrews et al.*, 1987] and that $\partial \bar{u}/\partial x$ as well as $\partial \bar{u}/\partial z$ are sometimes sufficiently large to affect the wave structure around the tropopause over Indonesia. Observational data are still quite limited to allow understanding the transport and photochemistry around the tropical tropopause comprehensively.

7. Conclusion

We have conducted an intensive observation with ozonesondes and rawinsondes in Indonesia in May and June 1995 to investigate the phenomenon of ozone enhancement in the tropical upper troposphere. We have obtained a temporal transition of the phenomenon that continued for about 20 days concurring with downward displacement of air as recognized from the variation of potential temperature. The concurrent prevailing meteorological feature was a zonal wind oscillation associated with the activity of the equatorial Kelvin wave around the tropopause and the Madden-Julian oscillation in the troposphere.

The detailed mechanism of the downward transport of ozone could be interpreted as follows: (1) Downward displacement associated with the Kelvin wave around the tropopause, 15-19 km, and the subsidence during the nonconvective phase of the MJO below 15 km had caused ozone transport from the lower stratosphere into the troposphere from May 9 to May 26; (2) the air mixing due to the Kelvin wave breaking occurred in the lowermost stratosphere and at the tropopause over Indonesia to cause the maximum ozone concentration around the tropopause on May 22; and (3) the ozone concentration in the uppermost troposphere had stopped increasing after May 22, and most of the ozone transported from the stratosphere had spread into the surrounding troposphere due to the horizontal mixing. These ozone-transporting processes are summarized in Figure 9.

The net amount of ozone transported from the stratosphere into the troposphere was estimated to be 9.9 DU as the upper limit. The horizontal extent of the ozone-increased region was $L_x \geq 6.6 \times 10^6$ m and $L_y \simeq 1.8 \times 10^6$ m. It should be emphasized that the ozone transport associated with the equatorial Kelvin wave activity including wave breaking and the MJO has the potential to affect the photochemistry in the tropical troposphere and lower stratosphere.

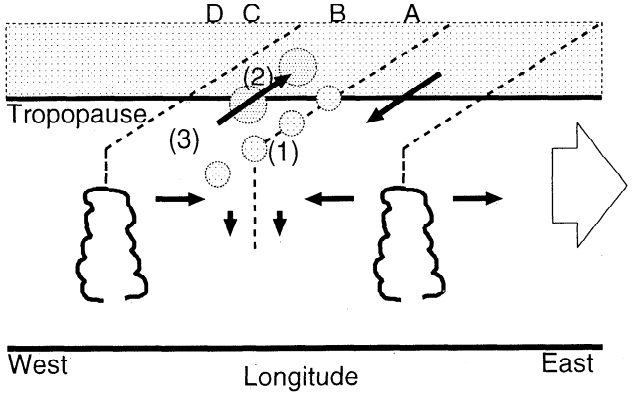

Figure 9. Schematic illustration of the longitude-altitude cross section of the observed ozone-transporting eastward moving system. The locations of 0 m s^{-1} zonal wind are indicated by bold dotted lines. Ozone-increased regions are shown by shaded circles. The letters A-D indicate the time when the phase of the system passed over the observation sites: A, between May 6 and 11; B, between May 15 and 16; C, between May 21 and 22; and D, May 26. The ozone-transporting processes were interpreted as follows: 1, downward motion associated with the Kelvin wave and the MJO; 2, air mixing due to the Kelvin wave breaking; and 3, horizontal mixing in the troposphere.

Acknowledgments. We deeply appreciate the extensive collaboration of Slamet Saraspriya and his staff at the Watukosek stratospheric balloon observatory of LAPAN. We also deeply thank Toshitaka Tsuda at Radio Atmospheric Science Center, Kyoto University, for providing the rawinsonde data at Bandung and for helpful discussions; K. Wada at the Center for the Climate System Research, University of Tokyo, for processing the GANAL data; and T. Nakazawa at the Meteorological Research Institute in Japan, for providing the GMS data. We are also deeply indebted to T. Imamura, N. Nishi, T. Horinouchi, N. Iwagami, and two anonymous reviewers for helpful comments and suggestions. The figures (except for 9) and plates were produced with the GFD-DENNOU Library. M.F. has been supported by research fellowships of the Japan Society for the Promotion of Science for Young Scientists since April 1998.

References

Andrews, D. G., J. R. Holton, and C. B. Leovy, *Middle Atmosphere Dynamics,* 489 pp., Academic, San Diego, Calif., 1987.

Crutzen, P., and M. Lawrence, Ozone clouds over the Atlantic, *Nature, 388,* 625-626, 1997.

Danielsen, E. F., A dehydration mechanism for the stratosphere, *Geophys. Res. Lett., 9,* 605-608, 1982.

Danielsen, E. F., In situ evidence of rapid, vertical, irreversible transport of lower tropospheric air into the lower tropical stratosphere by convective cloud turrets and by larger-scale upwelling in tropical cyclones, *J. Geophys. Res., 98,* 8665-8681, 1993.

Diab, R. D., et al., Vertical ozone distribution over southern Africa and adjacent oceans during SAFARI-92, *J. Geophys. Res., 101,* 23,823-23,833, 1996.

Fishman, J., C. E. Watson, J. C. Larsen, and J. A. Logan, Distribution of tropospheric ozone determined from satellite data, *J. Geophys. Res., 95,* 3599-3617, 1990.

Folkins, I., R. Chatfield, D. Baumgardner, and M. Proffitt, Biomass burning and deep convection in southeastern Asia: Results from ASHOE/MAESA, *J. Geophys. Res., 102,* 13,291-13,299, 1997.

Fujiwara, M., K. Kita, T. Ogawa, N. Komala, S. Saraspriya, A. Suripto, and T. Sano, Total ozone enhancement in September and October 1994 in Indonesia, paper presented at the XVIII Quadrennial Ozone Symposium, Int. Ozone Commiss., L'Aquila, Italy, September 12-21, 1996.

Holton, J. R., *An Introduction to Dynamic Meteorology,* 3rd ed., 511 pp., Academic, San Diego, Calif., 1992.

Holton, J. R., P. H. Haynes, M. E. McIntyre, A. R. Douglass, R. B. Rood, and L. Pfister, Stratosphere-troposphere exchange, *Rev. Geophys., 33,* 403-439, 1995.

Kley, D., P. J. Crutzen, H. G. J. Smit, H. Vömel, S. J. Oltmans, H. Grassl, and V. Ramanathan, Observations of near-zero ozone concentrations over the convective Pacific: Effects on air chemistry, *Science, 274,* 230-233, 1996.

Komala, N., S. Saraspriya, K. Kita, and T. Ogawa, Tropospheric ozone behavior observed in Indonesia, *Atmos. Environ., 30,* 1851-1856, 1996.

Madden, R. A., and P. R. Julian, Description of global-scale circulation cells in the tropics with a 40-50 day period, *J. Atmos. Sci., 29,* 1109-1123, 1972.

Maruyama, T., Annual and QBO-synchronized variations of lower-stratospheric equatorial wave activity over Singapore during 1961-1989, *J. Meteorol. Soc. Jpn., 69,* 219-232, 1991.

Nakazawa, T., Tropical super clusters within intraseasonal variations over the western Pacific, *J. Meteorol. Soc. Jpn., 66,* 823-839, 1988.

Newell, R. E., Y. Zhu, E. V. Browell, W. G. Read, and J. W. Waters, Walker circulation and tropical upper tropospheric water vapor, *J. Geophys. Res., 101,* 1961-1974, 1996.

Nishi, N., and A. Sumi, Eastward-moving disturbance near the tropopause along the equator during the TOGA COARE IOP, *J. Meteorol. Soc. Jpn., 73,* 321-337, 1995.

Pickering, K. E., A. M. Thompson, W.-K. Tao, and T. L. Kucsera, Upper tropospheric ozone production following mesoscale convection during STEP/EMEX, *J. Geophys. Res., 98,* 8737-8749, 1993.

Russell, P. B., L. Pfister, and H. B. Selkirk, The tropical experiment of the Stratosphere-Troposphere Exchange Project (STEP): Science objectives, operations, and summary findings, *J. Geophys. Res., 98,* 8563-8589, 1993.

Sato, K., and T. J. Dunkerton, Estimates of momentum flux associated with equatorial Kelvin and gravity waves, *J. Geophys. Res., 102,* 26247-26261, 1997.

Sato, K., F. Hasegawa, and I. Hirota, Short-period disturbances in the equatorial lower stratosphere, *J. Meteorol. Soc. Jpn., 72,* 859-872, 1994.

Shimizu, A., and T. Tsuda, Characteristics of Kelvin waves and gravity waves observed with radiosondes over Indonesia, *J. Geophys. Res., 102,* 26,159-26,171, 1997.

Suhre, K., J.-P. Cammas, P. Nédelec, R. Rosset, A. Marenco, and H. G. J. Smit, Ozone-rich transients in the upper equatorial Atlantic troposphere, *Nature, 388,* 661-663, 1997.

Thompson, A. M., W.-K. Tao, K. E. Pickering, J. R. Scala, and J. Simpson, Tropical deep convection and ozone formation, *Bull. Am. Meteorol. Soc., 78,* 1043-1054, 1997.

Trenberth, K. E., Storm tracks in the southern hemisphere, *J. Atmos. Sci., 48,* 2159-2178, 1991.

Tsuda, T., Y. Murayama, H. Wiryosumarto, S. W. B. Harijono, and S. Kato, Radiosonde observations of equatorial atmosphere dynamics over Indonesia, 1, Equatorial waves and diurnal tides, *J. Geophys. Res., 99,* 10,491-10,505, 1994a.

Tsuda, T., Y. Murayama, H. Wiryosumarto, S. W. B. Harijono, and S. Kato, Radiosonde observations of equatorial atmosphere dynamics over Indonesia, 2, Characteristics of gravity waves, *J. Geophys. Res., 99,* 10,507-10,516, 1994b.

Weller, R., R. Lilischkis, O. Schrems, R. Neuber, and S. Wessel, Vertical ozone distribution in the marine atmosphere over the central Atlantic Ocean (56°S-50°N), *J. Geophys. Res., 101,* 1387-1399, 1996.

Ziemke, J. R., and J. L. Stanford, Kelvin waves in total column ozone, *Geophys. Res. Lett., 21,* 105-108, 1994.

M. Fujiwara and K. Kita, Department of Earth and Planetary Physics, Graduate School of Science, University of Tokyo, Tokyo 113, Japan. (e-mail: fuji@sunep1.geoph.s.u-tokyo.ac.jp; kita@sunep1.geoph.s.u-tokyo.ac.jp)

T. Ogawa, Earth Observation Research Center, National Space Development Agency of Japan, Tokyo 106, Japan. (e-mail: t_ogawa@eorc.nasda.go.jp)

(Received November 12, 1997; revised April 21, 1998; accepted April 22, 1998.)